

# Performance Analysis of Low-Power Tokamak Reactors Using Predictive Integrated Modeling Code

**Y. Pianroj, S. Suwanna, and T. Onjun**

School of Manufacturing Systems and Mechanical Engineering  
Sirindhorn International Institute of Technology, Thammasat University,  
Pathum Thani, 12121, Thailand  
Email: thawatchai@siit.tu.ac.th

## Abstract

An investigation of plasma performance for a low-power tokamak reactors proposed by G.O. Ludwig [the 22<sup>nd</sup> Fusion Energy Conference, 2008, TH/P-3] is carried out using predictive integrated modeling codes BALDUR and TASK/TR. Simulations with the same plasma and boundary conditions from both codes are compared. There are three possible choices of core transport codes used in this study: a semi-empirical based Mixed Bohm/gyro-Bohm model, a theory-based Multimode model and a theory-based Current Diffusive Ballooning Mode model. It was found that the simulation results are quite pessimistic, except those using the Current Diffusive Ballooning Mode model in which a central temperature of above 20 keV was achieved. The sensitivity of the simulation results for plasma engineering parameters such as plasma current and heating power is also carried out. It is found that the performance is improved significantly with the increasing of the plasma current, however the effect of increasing the heating power on the performance improvement is less significant than that of increasing the plasma current.

**Keywords:** Tokamak; Low-power tokamak; BALDUR, TASK/TR

## 1. Introduction

Nuclear fusion is a possible energy source to be used in power plants. The concept of nuclear fusion has long been explored for a long time in many countries. Nuclear fusion processes involve a different set of nuclei from those in fission processes. Specifically, nuclear fission involves splitting heavy nuclei such as  $^{235}\text{U}$ . On the other hand, nuclear fusion involves fusing of light nuclei, such as hydrogen ( $H$ ) and its isotopes deuterium ( $D$ ) and tritium ( $T$ ).

There are several advantages of nuclear fusion power: abundant fuel reserves, low environmental impact, and high safety. On the other hand, there are also several disadvantages to fusion that must be considered, such as new technology is required for reaction controls. Specifically, to burn deuterium and tritium, it requires an ability to heat the fuel to the astounding temperature of several hundred million degrees Kelvin, which is much higher than the temperature at the center of the sun. [1]. An alternative approach to achieve steady

nuclear fusion power has been developed to demonstrate the power production in a compact reactor with low first wall load [2]. A low aspect ratio tokamak with high toroidal field seems to be an ideal candidate. To analyze this alternative approach, the figure of merit for tokamak is used to analyze the performance of low-power tokamak reactor proposed by G.O. Ludwig [3]. This figure of merit defines the performance of tokamak reactors in a simple way. It allows a search for sets of machine parameters that satisfy the performance goal, and to classify different tokamaks by their figure of merit values. One of the effective ways to validate the correctness of this approach is to put the set of tokamak parameters into an integrative modeling code.

In this work, a set of tokamak plasma parameters obtained from the analysis using the figure of merit concept is used to carry out an evolution of plasma, including temperature, current, and density, which are done via either BALDUR or TASK/TR predictive integrated modeling codes. The codes make use of a combination of anomalous and neoclassical transport models. The anomalous core transport is calculated by either the semiempirical Mixed Bohm/gyro-Bohm (mixed B/gB) model, the theory-based Multimode (MMM95) model, or the theory-based Current Diffusive Ballooning Mode (CDBM) model. For neoclassical transport, an NCLASS module is used in this work. Mixed B/gB and MMM95 models are used with BALDUR simulations. Mixed B/gB and CDBM models are used with TASK/TR simulations.

This paper is organized as follows: brief description of the analysis using figure of merit and integrated predictive modeling codes (BALDUR and TASK/TR) including the anomalous transport are given in section 2; the predictions of a low-power tokamak for Gerson's model are presented and discussed in section 3; sensitivity analysis is

found in section 4; and a summary is given in section 5.

## 2. The approaches to analyze the performance of a tokamak reactor

### 2.1 A figure of merit

A figure of merit evaluates the performance of a tokamak by considering the fusion power, fusion gain and average wall load. This method is based on a simple global model with the conduction and convection losses modeled by empirical scaling laws. The plasma model includes geometrical aspects, profiles and impurities effects, neoclassical effects, and stability constraints. Stability issues related to the toroidal beta limit, safety factor and density limit are taken into account. Then, a convenient normalization of the plasma temperature and density, and of the auxiliary power, is introduced, which leads to the definition of a figure of merit (X) and Cordy pass in G.O. Ludwig paper [3]. It is possible to search for sets of machine parameters that satisfy the performance goal. Consider a low-power tokamak reactor with a figure of merit of  $X=0.6$ . This tokamak produces 25 MW of fusion power, 500 kW/m<sup>2</sup> of power load on the closest wall, and operates along the Cordey pass; furthermore, a dimensionless figure of merit, which is independent of auxiliary power is defined by the exponent of the net heating power in the scaling law, which is assumed to be of the general form of the ITER IPB98(y,2); finally, the estimation of successful reactor conditions is given by the ratio  $Q$  (also called Fusion  $Q$ ) leng greater than or equal to 1.24. Hence, a list of possible machine parameters that satisfy the requirements are shown in Table 1 and Fusion  $Q$  is defined as equation (1).

$$\text{Fusion } Q = \frac{5 \times P_{\alpha, \text{ave}}}{P_{\text{OH}} + P_{\text{AUX}} + P_{\text{RAD}}} \quad (1)$$

where,  $P_{\alpha,avg}$  is the average of the alpha heating power during the last 50 seconds of simulation time (250-300 sec).  $P_{OH}$  is the ohmic heating power,  $P_{AUX}$  is the auxiliary heating power and  $P_{RAD}$  is the radiation loss power.

**Table 1** Main parameters of a possible low-power tokamak reactor.

Parameter (unit)	Value	Description
$R$ (m)	1.89	Major radius
$a$ (m)	0.94	Minor radius
$B_0$ (T)	3.6	Magnetic field
$I_p$ (MA)	10.0	Plasma current
$q^*$	2.01	Safety factor
$n_{20}$ ( $10^{20} m^{-3}$ )	1.33	Particle density
$\kappa$	2.0	Elongation
$\delta$	0.4	Triangularity

## 2.2 Integrated Predictive Modeling Code

### 2.2.1 BALDUR Code

BALDUR integrated predictive modeling code [4] is used to compute the time evolution of plasma profiles, including electron and ion temperatures, deuterium and tritium densities, helium and impurity densities, magnetic  $q$ , neutrals, and fast ions. These time-evolving profiles are computed in BALDUR integrated predictive modeling code by combining the effects of many physical processes self-consistently, including the effects of transport, plasma heating, particle influx, boundary conditions, the plasma equilibrium shape, and sawtooth oscillations. Fusion heating and helium ash accumulation are computed self-consistently. BALDUR simulations have been intensively compared against various plasma experiments, which yield an overall agreement of 10% RMS deviation [5, 6]. In BALDUR code, fusion heating power is determined using the nuclear reaction rates and a Fokker Planck package to compute the slowing down spectrum of fast alpha

particles on each flux surface in the plasma. The fusion heating component of BALDUR code also computes the rate of production of thermal helium ions and the rate of depletion of deuterium and tritium ions within the plasma core. Brief details of these transport models are described below.

### 2.2.2 TASK/TR Code

TASK/TR code [7] can calculate the main features, as below:

- By using the diffusive transport equations, it calculates a temporal evolution of the density and temperature for every species of particle in a core plasma: electrons, deuteriums, tritiums, thermalized  $\alpha$  particles, neutrals, multiple impurities, and the other particles. The code also deals with a local evolution for the two kinds of beam ions associated with the heating by fast  $\alpha$  particles and neutral beam injections.
- Analysis including neutral beam injections heating current drive, pellet injection and current ramp up is also possible and it can evaluate quantitatively a plasma response to these external actuators.
- Since the transport equations include various geometric factors, it is easy to carry out a transport simulation coupled with two-dimensional equilibrium code.
- The code may incorporate experiment data through standard databases.
- A lot of turbulent and neoclassical transport models have been implemented in the code.

TASK/TR code solves a one-dimensional diffusive equations for densities, temperature, and a poloidal magnetic flux with respect to the normalized minor radius,  $\rho$  [8]. The effect of  $\vec{E} \times \vec{B}$  shear stabilization is considered to be important to allow a plasma to form a transport barrier. Applying this effect appropriately for simulation, TASK/TR code calculates the radial electric field, which is derived from the radial ion force

balance. It should be noted that toroidal velocity data is unavailable in some discharges. Therefore, we multiply the toroidal angular speed by the surface averaged geometrical major radius, both of which are usually included in the database. The poloidal velocity is computed using the NCLASS module. Moreover, TASK/TR code includes various neoclassical transport models to evaluate the transport coefficients, the bootstrap current, the neoclassical resistivity and the poloidal flow velocity and viscosity. The theory-based turbulent transport model, the CDBM model, is included in TASK/TR. A brief description of the core transport models is given in the following section.

### 2.2.3 Core transport model

#### 2.2.3.1 Mixed B/gB core transport model

The Mixed B/gB core transport model [9] is an empirical transport model. It was originally a local transport model with Bohm scaling. A transport model is said to be “local” when the transport fluxes (such as heat and particle fluxes) depend entirely on local plasma properties (such as temperatures, densities, and their gradients). A transport model is said to have “Bohm” scaling when the transport diffusivities are proportional to the gyro-radius times thermal velocity over a plasma linear dimension such as major radius. Transport diffusivities in models with Bohm scaling are also functions of the profile shapes (characterized by normalized gradients) and other plasma parameters such as magnetic  $q$ , which are all assumed to be held fixed in systematic scans in which only the gyro-radius is changed relative to plasma dimensions. The original JET model was subsequently extended to describe ion transport, and a gyro-Bohm term was added in order for simulations to be able to match data from smaller tokamaks as well as data from larger machines. A transport model is said to have “gyro-Bohm” scaling when the

transport diffusivities are proportional to the square of the gyroradius times thermal velocity over the square of the plasma linear dimension. The Bohm contribution to the JET model usually dominates over most of the radial extent of the plasma. The gyro-Bohm contribution usually makes its largest contribution in the deep core of the plasma and plays a significant role only in smaller tokamaks with relatively low power and low magnetic field. The Mixed B/gB transport model can be expressed as follows[10]:

$$\chi_e = 1.0\chi_{gB} + 2.0\chi_B$$

$$\chi_i = 0.5\chi_{gB} + 4.0\chi_B + \chi_{neo}$$

$$D_H = [0.3 + 0.7\rho] \frac{\chi_e \chi_i}{\chi_e + \chi_i}$$

$$D_z = D_H$$

where,

$$\chi_{gB} = 5 \times 10^{-6} \sqrt{T_e} \left| \frac{\nabla T_e}{B_\phi^2} \right|,$$

$$\chi_B = 4 \times 10^{-5} R \left| \frac{\nabla(n_e T_e)}{n_e B_\phi} \right| q^2 \left( \frac{T_{e,0.8} - T_{e,1.0}}{T_{e,1.0}} \right) \times \Theta \left( -0.14 + s - \frac{1.47\omega_{E \times B}}{\gamma_{ITG}} \right)$$

where,  $\chi_e$  is the electron diffusivity ( $m^2/s$ ),  $\chi_i$  is the ion diffusivity ( $m^2/s$ ),  $D_H$  is the particle diffusivity ( $m^2/s$ ),  $D_z$  is the impurity diffusivity ( $m^2/s$ ),  $\chi_{gB}$  is the gyro-Bohm contribution,  $\chi_B$  is Bohm contribution,  $\rho$  is normalized minor radius,  $T_e$  is the electron temperature (keV),  $B_\phi$  is the toroidal magnetic field (Tesla),  $R$  is the major radius (m),  $n_e$  is the local electron density ( $m^{-3}$ ),  $q$  is the safety factor,  $s$  is the magnetic shear,  $\omega_{E \times B}$  is the flow shearing rate,  $\Theta$  is a Heaviside step function, and  $\gamma_{ITG}$  is the ion temperature gradient (ITG) growth rate, estimated as  $v_{ti}/qR$ , in which  $v_{ti}$  is the ion thermal velocity.

#### 2.2.3.2 Multi-Mode core transport model

Multi-Mode Model (MMM95) is a combination of theory-motivated transport

models used to predict plasma profiles in tokamaks. It consists of the Weiland model for the ion temperature gradient (ITG) and trapped electron modes (TEM)[11], the Guzdar-Drake model for drift-resistive ballooning modes [12, 13], and kinetic ballooning modes[14]. Usually, the Weiland model for drift modes provides the largest contribution, followed by the drift-resistive ballooning mode and the kinetic ballooning mode. The Weiland model ( $\chi_{Weiland}$ ) is derived by linearizing the fluid equations, with magnetic drifts for each plasma species. Eigenvalues and eigenvectors computed from these fluid equations are then used to compute a quasi-linear approximation for the thermal and helium transport fluxes. The Weiland model includes many different physical phenomena such as effects of trapped electrons, unequal ion and electron temperatures, impurities, fast ions, finite  $\beta$  and collisions. The resistive ballooning model ( $\chi_{RB}$ ) in MMM95 transport model is based on the 1993  $\vec{E} \times \vec{B}$  drift-resistive ballooning mode model by Guzdar-Drake, in which the transport is proportional to the pressure gradient and collisionality. The contribution from the resistive ballooning model usually dominates the transport near the plasma edge. The kinetic ballooning model ( $\chi_{KB}$ ) is a semi-empirical model, which usually provides a small contribution to the total diffusivity throughout the plasma, except near the magnetic axis. However, in this work, it is found that the contribution from the kinetic ballooning model plays quite a significant role in the region near the plasma core up to a radius of 1.0 m. This model is an approximation to the first ballooning mode stability limit. All the anomalous transport contributions to the MMM95 transport model are multiplied by  $\kappa^{-4}$  since the models were originally derived for circular plasmas. The expressions of transport coefficients in MMM95 are:

$$\begin{aligned}\chi_i &= 0.8\chi_{iITG\&TEM} + 1.0\chi_{iRB} + 1.0\chi_{iKB} \\ \chi_e &= 0.8\chi_{eITG\&TEM} + 1.0\chi_{eRB} + 1.0\chi_{eKB} \\ D_H &= 0.8D_{HITG\&TEM} + 1.0D_{HRE} + 1.0D_{HKB} \\ D_z &= 0.8D_{zITG\&TEM} + 1.0D_{zRE} + 1.0D_{zKB}\end{aligned}$$

where  $\chi_e$  is the electron diffusivity,  $\chi_i$  is the ion diffusivity,  $D_H$  is the particle diffusivity,  $D_z$  is the impurity diffusivity,  $\chi_{ITG\&TEM}$  is the thermal diffusivity of ion temperature gradient and trapped electron mode,  $\chi_{RB}$  is the resistive ballooning thermal diffusivity and  $\chi_{KB}$  is the kinetic ballooning thermal diffusivity.

### 2.2.3.3 Current Diffusive Ballooning Mode

The CDBM model is based on the theory of self-sustained turbulence due to the ballooning mode [15, 16] driven by the turbulent current diffusivity. Inclusion of the electron viscosity, which has often been neglected in a conventional MHD theory allows the electromagnetic fluctuation to enhance electron viscosity and to make instabilities more unstable in a short-wavelength mode. As the fluctuation amplitude increases, however, the stabilizing effect due to the thermal diffusivity and the ion viscosity eventually overcomes the destabilizing effect of the current diffusivity. The saturation level is determined by the balance of these effects. By solving an eigenvalue problem for the ballooning mode, a general expression of the turbulent thermal diffusivity [17] can be obtained:

$$\chi_{CDBM} = CF(s, \alpha)\alpha^{3/2} \frac{c^2 v_A}{\omega_{pe}^2 qR}$$

here,  $C = 12$ , is a fitting parameter,  $c$  is the speed of light (m/s),  $\omega_{pe}$  is the electron plasma frequency (Hz),  $v_A$  is the toroidal Alfvén velocity (m/s), and  $q$  is the safety factor. The factor  $F$  is a function of the magnetic shear  $s$  and the normalized MHD pressure gradient  $\alpha$  defined by:

$$s \equiv \frac{r dq}{q dr}$$

$$\alpha \equiv -q^2 R \frac{d\beta}{dr}$$

where  $r$  is defined as the midplane minor radius and  $\beta$  is the ratio of the plasma pressure to the magnetic pressure,  $(p_e + p_i)/(B_0^2/2\mu_0)$ . The definition of the  $F$  is given by

$$F = \begin{cases} \frac{1}{\sqrt{2(1-2s)(1-2s'+3s^2)}}, & \text{for } s' = s - \alpha < 0 \\ \frac{(1+9\sqrt{2s^2})}{\sqrt{2(1-2s'+3s^2+2s^3)}}, & \text{for } s' = s - \alpha > 0 \end{cases}$$

The effect of the magnetic curvature is neglected because the original formula is included in the large aspect ratio approximation. The fitting parameter,  $C=12$ , is determined by comparing the energy confinement time for the standard plasma parameter with the ITER-89P L-mode scaling law.

### 3. Simulation Results and Discussions

BALDUR code with either Mixed B/gB or MMM95 core transport model as well as TASK/TR with either Mixed B/gB or CDBM core transport model are used to carry out simulations of a low-power tokamak reactor which is based on the Gerson's design concept. The input parameters for the two integrated predictive modeling codes are given in Table 1. In the simulations, the plasma density are slowly ramped up in the first 100 sec, after that it reaches to the target, and the plasma density is maintained throughout the simulation period. The plasma current during the start up phase is initially 1 MA to 10 MA. Then, it is maintained at this target along the simulation period from 200 to 300 sec. Thus, the current target will be tested at 10 MA. Moreover the power auxiliaries come

from Neutral Beam Injection (NBI) equal to 13 MW and Radio Frequency Heating equal to 10 and 20 MW. In addition these auxiliary power sources were combined with the ohmic heating that is generated from the plasma current.

In this work, the density and temperature which are predicted (Mixed B/gB) at time 298 sec will be used as initial conditions for TASK/TR, because TASK/TR is given the fixed density profile throughout the simulation in these forms:

$$n(\rho) = (n_0 - n_s)(1 - \rho^{n_1})^{n_2} + n_s \quad (2)$$

where,  $n_0$  is the density at the magnetic axis,  $n_s$  is the density at the edge,  $n_1$ , and  $n_2$  are the exponents. In Figure 1, the profiles of electron and ion temperature as a function of normalized minor radius ( $\rho$ ) with plasma current 10 MA at time 295 sec are plotted. The auxiliary power is set to 23 (RF 10 MW + NBI 13 MW) and 33 MW (RF 20 MW + NBI 13 MW). Note that the plasma has already reached a steady state at this time. These results are shown for simulations that are carried out using BALDUR with Mixed B/gB, BALDUR with MMM95, TASK/TR with Mixed B/gB and TASK/TR with CDBM core transport models. The results of the electron and ion temperature at plasma core and at the plasma edge are shown in Table 2. It can be seen that the electron and ion temperature at the plasma edge are started at an initial point around 1.81 keV, with the plasma current equal to 10 MA. Then, the temperatures are ramped up to the maximum temperatures at the plasma core. The rate of temperature ramp up is due to the difference of core transport models that control the transport phenomena inside the tokamak plasma. It can be seen in Figure 1 and Table 2 that increasing the auxiliary power from 23 MW to 33 MW caused a higher temperature inside the tokamak plasma. This means that the electron core temperature increases by 305%, 205%,

320% and 516% when the auxiliary power is increased in the simulations using the MMM95 (BALDUR), Mixed B/gB (BALDUR), Mixed B/gB (TASK/TR), and CDBM (TASK/TR), respectively. Never-

theless the results that were carried from CDBM (TASK/TR) core transport model showed optimistic electron and ion temperatures.

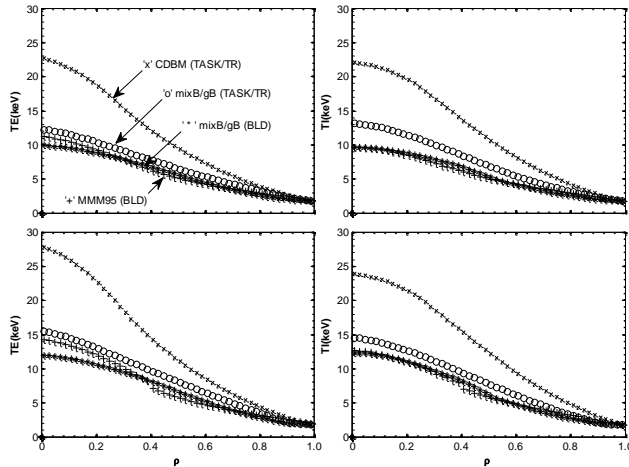


**Figure 1** Profile of electron and ion temperature as a function of normalized minor radius at time 295 sec with plasma current equal to 10 MA, with auxiliary power equal to 23 MW (upper panels) and 33 MW (lower panels).

**Table 2** Summary of electron and ion temperature at the core ( $T_0$ ) and edge ( $T_{edge}$ ) of plasma at time 295 sec of simulation.

Plasma current (MA)/ $P_{aux}$ (MW)	Transport Model	$T_e$		$T_i$	
		$T_0$ (keV)	$T_{edge}$ (keV)	$T_0$ (keV)	$T_{edge}$ (keV)
10/23	MMM95 (BLD)	11.16	1.90	9.60	1.81
	Mixed B/gB (BLD)	9.92	1.81	9.60	1.80
	Mixed B/gB (TASK/TR)	12.20	1.72	13.10	1.71
	CDBM (TASK/TR)	22.66	1.74	22.10	1.75
10/33	MMM95 (BLD)	14.21	1.94	12.60	1.82
	Mixed B/gB (BLD)	11.97	1.82	12.31	1.80
	Mixed B/gB (TASK/TR)	15.40	1.78	14.51	1.75
	CDBM (TASK/TR)	27.76	1.77	23.84	1.78

In Figure 2 the electron and ion density profiles are plotted as a function of normalized minor radius. As mentioned

above, the density of TASK/TR is fixed by Equation (2) thus, the electron density

profiles are assumed with Equation (4) in  $10^{20} \text{ m}^{-3}$ .

$$n_e = n_D + n_T + (2 \times n_{He}) \quad (4)$$

where,  $n_e$ ,  $n_D$ ,  $n_T$ , and  $n_{He}$  are the on-axis density for electron, deuterium, tritium and helium, respectively. For electron density, the profiles fit very well with the electron densities that are predicted by BALDUR code; however, the electron and ion density profiles are calculated by MMM95 core transport model. It can be seen that the shape of both profiles are a small hump in the region of about 60% of plasma [18].

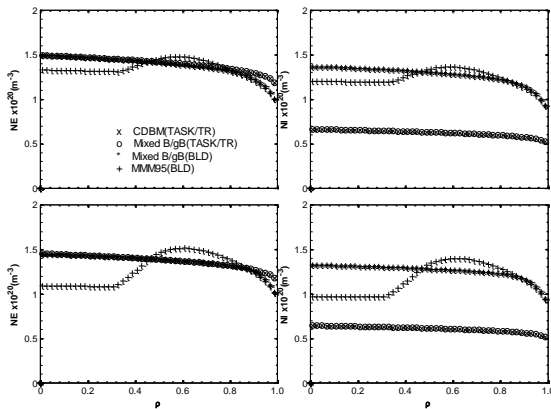


**Figure 2** Profile of electron and ion density as a function of normalized minor radius at time 295 sec with plasma current equal to 10 MA, with auxiliary power equal to 23 MW (upper panels) and 33 MW (lower panels).

For the concept of D-T thermonuclear fusion, the thermonuclear power consists of two parts. Four fifths of the reaction energy is carried by the neutrons and the remainder is carried by the alpha particles. The neutrons leave the plasma without interaction, but the  $\alpha$ -particles, being charged, are confined by the magnetic field. The  $\alpha$ -particles will transfer their energy to the plasma through collisions. Moreover the total energy which is confined in the plasma is named then stored energy. Thus, the  $\alpha$ -power and stored energy

represent the thermonuclear fusion reaction. The tokamak performance or the power, the parameter which defines the ratio between the power produced by the thermonuclear fusion reaction and the power supplied by the external heating devices is called “Fusion  $Q$ ”. It is shown in equation (1), if Fusion  $Q = 1$ , then the power produced by nuclear fusion is equal to the power provided by the external heating devices. The alpha power and the stored energy as a function of time are calculated by integrated predictive modeling codes BALDUR and TASK/TR with different core transport models MMM95, mixed B/gB, and CDBM as shown in Figure 3. Furthermore, the summary of average alpha power, average of stored energy and Fusion  $Q$  during the last 50 second (250-300 sec) of the simulation time are shown in Table 4. It can be seen that the plasma current is equal to 10 MA. Only the CDBM core transport model, in TASK/TR code predicted a simulation result that reaches to the Gerson’s Fusion  $Q$  target of around 1.

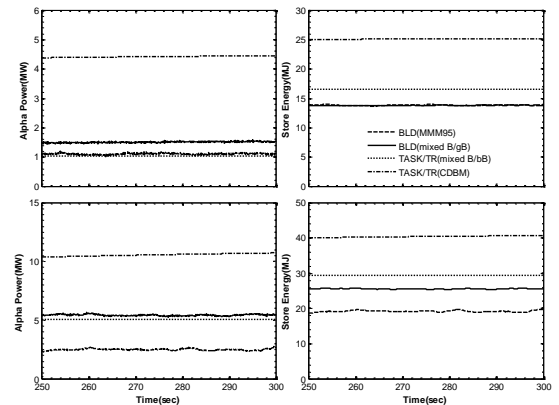


**Figure 3** The alpha power and store energy as a function of time from 250-300 sec when the ohmic heating comes from the plasma current (10 MA) and auxiliary heating power 23 MW (upper panels), and 33 MW (lower panels).

## 4. Sensitivity Study

As described in Section 3 about the heating system of a tokamak, the increase in auxiliary heating does not significantly affect the Fusion  $Q$ . On the other hand, if the plasma current increases, the Fusion  $Q$  will increase extensively. This is the hypothesis of this section. The initial plasma current is 1.0 MA, and it is maintained at a target value of 15 MA during 200 to 300 sec. The auxiliary heating power is set to 23 and 33 MW. It can be seen in Figure 4 and Table 3 that the increase of auxiliary power from 23 MW to 33 MW caused the temperature to increase inside the tokamak plasma. They are shown in Figure 5. The results show the same trend, similar to the case of 10 MA plasma current. The alpha power and stored energy during the last 50 seconds of the simulation are shown in Figure 6 and Table 4. In Figure 6, it shows higher magnitude of

alpha power and stored energy when compared with the previous case, due to the increasing of plasma current, which also causes an increased ohmic heating.

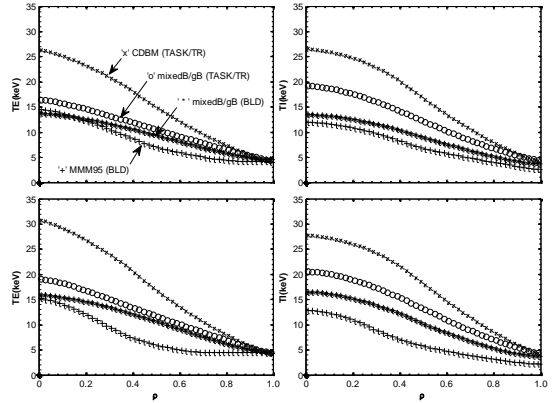


**Figure 4** Electron and ion temperature as functions of normalized minor radius at 295 sec with plasma current equal to 15 MA, with auxiliary power equaling to 23 MW (upper panels) and 33 MW (lower panels).

**Table 3** Summary of electron and ion temperature at the core ( $T_0$ ) and edge ( $T_{edge}$ ) of plasma at time 295 sec of simulation.

Plasma current (MA)/ $P_{aux}$ (MW)	Transport Model	$T_e$		$T_i$	
		$T_0$ (keV)	$T_{edge}$ (keV)	$T_0$ (keV)	$T_{edge}$ (keV)
15/23	MMM95 (BLD)	14.51	4.05	11.90	2.60
	Mixed B/gB (BLD)	13.73	4.55	13.41	3.74
	Mixed B/gB (TASK/TR)	16.33	4.30	19.14	4.36
	CDBM (TASK/TR)	26.31	4.29	26.58	4.28
15/33	MMM95 (BLD)	15.17	4.33	12.81	2.15
	Mixed B/gB (BLD)	15.90	4.56	16.50	3.76
	Mixed B/gB (TASK/TR)	19.02	4.30	20.51	4.25
	CDBM (TASK/TR)	30.72	4.31	27.80	4.31

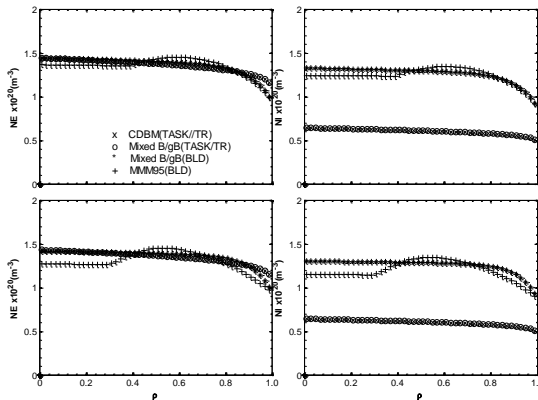


**Figure 5** Profile of electron and ion density as functions of normalized minor radius at 295 sec with plasma current equal to 15 MA, with auxiliary power equaling to 23 MW (upper panels) and 33 MW (lower panels).

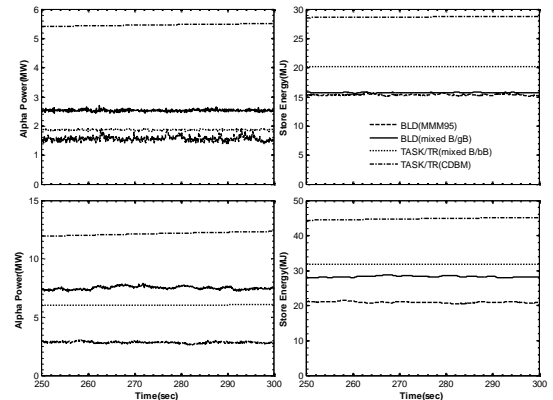


**Figure 6** The alpha power and stored energy as functions of time from 250-300 sec when the ohmic heating comes from the plasma current (15 MA), and auxiliary heating power 23 MW (upper panels), and 33 MW (lower panels).

**Table 4** Summary of average alpha power, stored energy, and Fusion  $Q$  during the last 50 sec (250-300 sec) of the simulation.

Parameter	Plasma current (MA)/ $P_{aux}$ (MW)	MMM95 (BLD)	mixed B/gB (BLD)	mixed B/gB (TASK)	CDBM (TASK)
Alpha power (MW)	10/23	1.10	1.50	1.03	4.41
	10/33	1.56	2.53	1.86	5.46
	15/23	2.48	5.42	5.06	10.50
	15/33	2.83	7.50	6.03	12.10
Stored energy (MJ)	10/23	13.80	13.77	16.47	25.08
	10/33	15.33	15.68	20.14	28.66
	15/23	19.15	25.51	29.27	40.35
	15/33	20.91	28.24	31.75	44.75
Fusion $Q$	10/23	0.19	0.26	0.21	0.94
	10/33	0.21	0.33	0.27	0.82
	15/23	0.36	0.80	1.03	2.23
	15/33	0.33	0.84	0.88	1.82

When the plasma current increased from 10 to 15 MA, high Fusion  $Q$  values (nearly 1) are obtained by both BALDUR and TASK/TR using the Mixed B/gB model. At 15 MA plasma current, TASK/TR with CDBM gives a Fusion  $Q$  of around 2, which achieves the Gerson's Fusion  $Q$  target of 1.24. It should be noted that the plasma current is the major heating element to achieve the Fusion  $Q$  target,

because it is significantly related to the alpha power production. Fusion  $Q$  predicted by BALDUR using MMM95 gives lower Fusion  $Q$  values because this version of multi-mode core transport model does not include the  $\vec{E} \times \vec{B}$  flow shear stabilization effect, which will stabilize the turbulent transport and form an internal transport barrier (ITB). When the ITB is formed, the

plasma performance will be improved [19, 20].

## 5. Conclusion

Fusion  $Q$  values predicted for low-power tokamak reactors are carried out using two integrated predictive modeling codes (BALDUR and TASK/TR) with the different core transport models MMM95, Mixed B/gB, and CDBM. Overall, Fusion  $Q$  that is predicted by this approach shows a result lower than that predicted by the theoretical base method from G.O. Ludwig design. The TASK/TR code with CDBM model predicted the highest performance. However, the Fusion  $Q$  can be improved by increasing the plasma current. However an increase of power auxiliary is not significant to achieved the performance goal.

## 6. Acknowledgments

This work is supported by the Thailand Research Fund (TRF) under Contract No.RMU5180017, and the Thailand National Research University Project.

Y. Pianroj thanks the Commission on Higher Education, Thailand for support under the program Strategic Scholarships for Frontier Research Network for the Ph.D. Program (Thai Doctoral degree), for this research.

## 7. References

- [1] Aymar R., Barabaschi P. and Shimonura Y., The ITER Design *Plasma Phys. Control. Fusion*, Vol. 44, p. 519, 2002.
- [2] Bateman G., Kritz A. H., Kinsey J. E., *et al.*, Predicting Temperature and Density Profiles in Tokamaks, *Phys. Plasmas*, Vol. 5, p. 1793, 1998.
- [3] Ludwig G. O., Andrade M. C. R., Gryaznevich M., *et al.*, Performance Analysis of Low-power Tokamak Reactors, Paper Presented in The 22<sup>nd</sup> IAEA Fusion Energy, Geneva, Switzerland, 2008.
- [4] Singer C. E., Post D. E. and Mikkelsen D. R., A One-dimension Plasma Transport Code, *Comput. Phys. Commun.*, Vol. 49, pp. 275-398, 1988.
- [5] Hannum D., Bateman G. and Kinsey J., Comparison of High-mode Predictive Simulations Using Mixed Bohm/gyro-Bohm and Multi-Mode MMM95 Transport Models, *Phys. Plasmas*, Vol. 8, p. 964, 2001.
- [6] Onjun T., Bateman G. and Kritz A. H., Comparison of Low Confinement Mode Transport Simulation Using Mixed Bohm/gyro-Bohm and the Multi-Mode 95 Transport Model, *Phys. Plasmas*, Vol. 8, p. 975, 2001.
- [7] Honda M., Transport Simulation of Tokamak Plasmas Including Plasma Rotation and Radial Electric Field, Ph.D. Thesis, Nuclear Engineering, Kyoto University, 2007.
- [8] Honda M. and Fukuyama A., Comparison of Turbulent Transport Models of L- and H-mode Plasmas, *Nuclear Fusion*, Vol. 46, pp. 580-593, 2006.
- [9] Tala T. J. J., Heikkinen J. A. and Parail V. V., ITB Formation in Term of  $W_{ExB}$  Flow Shear and Magnetic Shear on JET, *Plasma Phys. Control. Fusion*, Vol. 43, p. 507, 2001.
- [10] Onjun T. and Pianroj Y., Simulations of ITER with Combined Effects of Internal and Edge Transport Barriers, *Nuclear Fusion*, Vol. 49, p. 075003, 2009.
- [11] Weiland J. and Hirose A., Electromagnetic and Kinetic Effects on the Ion Temperature Gradient Mode, *Nuclear Fusion*, Vol. 32, p. 151, 1992.
- [12] Kinsey J. E., Bateman G., Kritz A. H., *et al.*, Comparison of Two Resistive Ballooning Mode Models in

- Transport Simulations, *Phys. Plasmas*, Vol. 3, p. 561, 1995.
- [13] Guzdar P. N., Drake J. F., Mccarthy D., *et al.*, Three-dimensional Fluid Simulations of the Nonlinear Drift-resistive Ballooning Modes in Tokamak Edge Plasmas, *Phys. Fluids B*, Vol. 5, p. 3712, 1993.
- [14] Bateman G., Kritiz A. H. and Kinsey J. E., Predicting Temperature and Density Profiles in Tokamaks, *Physics of Plasmas*, Vol. 5, p. 1793, 1998.
- [15] Itoh K., Yagi M., Itoh S. I., *et al.*, L-Mode Confinement Medel Based on Transport-MHD Theory in Tokamaks, *Plasma Phys. Control. Fusion*, Vol. 35, pp. 543-549, 1993.
- [16] Itoh K., Itoh S. I., Fukuyama A., *et al.*, Self-sustained Turbulence and L-mode Confinement in Toroidal Plasmas. I, *Plasma Phys. Control. Fusion*, Vol. 36, pp. 279-306, 1994.
- [17] Fukuyama A., Itoh K., Itoh S. I., *et al.*, Transport Simulation on L-Mode and Improved Confinement Associated with Current Profile Modification, *Plasma Phys. Control. Fusion*, Vol. 37, pp. 611-631, 1995.
- [18] Onjun T., Tharasrisuthi K., Pankin A. Y., *et al.*, Projected Performance of ITER Based on Different Theoretical Based Pedestal Temperature Models *J. Plasma Fusion Res. Series*, Vol. 123, p. 012034, 2008.
- [19] Beer M. A., Budny R. V., Challis C. D., *et al.*, Turbulence Suppression by ExB shear in JET Optimized Shear Pulses, Paper Presented in The 26<sup>th</sup> EPS Conf. on Contr. Fusion and Plasma Phys., Maastricht, 1999.
- [20] Burrell K. H., Effects of ExB Velocity Shear and Magnetic Shear on Turbulence and Transport in Magnetic Confinement Device, *Phys. Plasmas*, Vol. 4, p. 1499, 1997.